2016

Noise Effects In Capillary Tubes Caused By Refrigerant Flow

Thomas Tannert
Bitzer-Stiftungsprofessur für Kälte-, Kryo- und Kompressorentechnik / Technische Universität Dresden, Germany,
thomas.tannert@tu-dresden.de

Ullrich Hesse
Bitzer-Stiftungsprofessur für Kälte-, Kryo- und Kompressorentechnik / Technische Universität Dresden, Germany,
ullrich.hesse@tu-dresden.de

Noise Effects In Capillary Tubes Caused By Refrigerant Flow

Thomas TANNERT*, Ullrich HESSE

Technische Universität Dresden, Institut für Energietechnik,
Bitzer-Stiftungsprofessur für Kälte-, Kryo- und Kompressorentechnik,
Münchner Platz 3, 01062 Dresden, Germany
Thomas.Tannert@tu-dresden.de
Ullrich.Hesse@tu-dresden.de

* Corresponding Author

ABSTRACT

The preferred cooling process for household refrigeration appliances is a vapor compression refrigeration process with a capillary tube as expansion device. The vapor compression refrigeration system requires a phase change of the refrigerant inside the condenser and evaporator. The condenser outlet defines directly the refrigerant state at the capillary tube inlet through a direct connection of condenser outlet and capillary tube inlet. This is commonly practiced for household refrigeration systems. Due to unsteady operation conditions the refrigerant state can change from subcooled liquid to saturated liquid with partially a vapor phase at the capillary tube inlet. The refrigerant flow inside the capillary tube is either adiabatic or non-adiabatic (by utilizing internal heat exchange). In both cases the refrigerants state of matter changes during the expansion with an increase of vapor quality towards the capillary tube outlet. A variable vapor quality at the capillary tube inlet causes different flow patterns, especially at the capillary tube outlet. These flow patterns change periodically depending on the refrigerant state of matter at the capillary tube inlet. Associated with the periodical changing flow patterns the occurrence of noise effects with the same periodicity and remarkable variations of the sound pressure level can be observed at the capillary tube outlet.

This paper presents the experimental investigations on the simultaneous occurrence of refrigerant flow patterns and corresponding noise effects at the outlet of a capillary tube installed in a refrigeration test cycle. The discussion of the experimental results leads to an explanation of causal relation between distinguishable flow patterns and corresponding noise effects.

Keywords: refrigerator, capillary tube, flow pattern, two phase flow, noise

1. INTRODUCTION

Capillary tubes are often used as expansion device in refrigeration cycles with small cooling capacity. Compared with expansion valves they’re at a lower cost level and no maintenance is needed. Usually the control strategy of a domestic refrigerator is kept simple. Therefor the state variables of the cooling process are transient during operation. The varying conditions at capillary tube inlet and outlet cause a fluctuating mass flow rate through the capillary tube. The different flow patterns occurring in the capillary tube are discussed in Tannert and Hesse (2013). Corresponding to the alternating flow pattern a significant noise fluctuation can be observed during the operation of the refrigerator. Those circumstances are not accepted by the customers.

The aim of the investigations presented in this paper is to localize the noise excitation and to quantify the time-depending fluctuation of the noise’s amplitude. Therefor the utilized test setup and the methods of measurement are explained. Additionally the relationship to corresponding events in the refrigerant flow is figured out and the root-causes are discussed.

2. THEORETICAL ASPECTS

2.1. Origins of noise excitation

Basically it can be distinguished between flow-induced and mechanically excited noises. Flow-induced noises are caused by a locally occurring pressure fluctuation in the refrigerant flow. Mechanically excited noises are caused by a device with continuously or periodically moving components, for example the compressors or switchable valves. In both cases structure-born sound will be generated. All components of the refrigeration cycle are usually joined and mechanically fixed so that they're representing a reverberant structure. The vibration generated at one end of the structure is well conducted to components which tend to good emission of airborne noise. Therefore externally perceivable noises occur. Especially in household refrigerators the thermal insulation is made of polyurethane foam and thus it contributes to the structural sound transmission.

A two-phase refrigerant flow occurs in the heat exchangers and in particular in the capillary tube of the refrigeration circuit. The presence of gas or vapor bubbles in the refrigerant flow is the initial condition that condensation induced shocks (CIS) may occur in the refrigerant circuit. These shocks are caused by collapsing bubbles under certain thermal conditions. For those conditions a suitable arrangement of the piping is required, which usually is provided by refrigeration cycles with a suction line heat exchanger (SLHX). Here, the capillary tube is section-wise conducted with the suction gas line. The vapor mass fraction in the capillary tube's refrigerant flow increases towards the capillary tube outlet. With an increasing temperature difference between the suction gas line and the capillary tube the possibility of a bubble collapsing in the capillary tube refrigerant flow increases. For instance this scenario can occur short after the refrigeration cycle start-up as described in Hartmann and Melo (2012).

During the entrainment of liquid-only refrigerant in the capillary tube a thermal imbalance of the liquid phase can occur due to the thermal inertia and the high flow velocity. The superheated liquid refrigerant forms a metastable liquid phase due to the temporary absent of evaporation. The local end of the metastable liquid phase is characterized by the so-called flashpoint. During this phase the first vapor bubbles occur due to evaporation. The ongoing refrigerant flow is now in a metastable two-phase state. The delayed onset of evaporation is continued downstream until the thermodynamic state variables reaches their saturated values and the refrigerant flow turns into a thermal balanced two-phase flow. With the first upcoming vapor bubbles pressure surges, so-called evaporation strokes, can occur and can cause flow-induced noises. Simoes-Moreiraa and Bullard (2003) showed that there will be a periodic shift of this flashpoint inside the capillary tube, accompanied with a fluctuating mass flow rate, especially when variable speed compressors are used.

The dynamic behavior of vapor bubbles is used to analyze the peaks in the frequency response of the flow induced noise. In this case the resonance frequency of these bubbles is important. While passing an orifices or a flow section with sharply rising diameter, e.g. at the capillary tube outlet, the resonating vapor bubbles emitting sound waves. First investigations on this were carried out by Minnaert (1933) for free rising gas bubbles in liquid fluid, without constrains of the flow cross-section. Therein a dependency between the resonance frequency and the diameter of the spherical bubbles could be determined. The formal context is given in equation (1).

$$f_{res,spherical} = \frac{1}{\pi \cdot d}\sqrt{\frac{3 \cdot \kappa \cdot p}{\rho_{liq}}} \tag{1}$$

The localization of flow-induced noise in refrigeration cycles and the relation to changing flow pattern are described in Han *et al.* (2009). In this it could be observed, that an increase of the noise level occurs at the same time, as the flow pattern changes towards intermittent flow. The evaporator inlet was determined as the location, where the noise occurs. Equation (1) was first considered to be accurate for the explanation of the measured frequencies. Improvements for reducing the noise are presented in Han *et al.* (2010).

In a further study (Han *et al.*, 2011) it was figured out, that the applicability of equation (1) is not suitable to determine the resonance frequency of vapor bubbles in pipes. The geometry of bubbles in pipes is constrained by the tube wall. Therefore the bubbles cannot expand to a spherical shape. They rather expand to a cylindrical shape. This shape of an elongated bubble is also designated as Taylor bubbles. The sequence of several successive Taylor bubbles in a pipe and the geometric variables are shown in Figure 2.

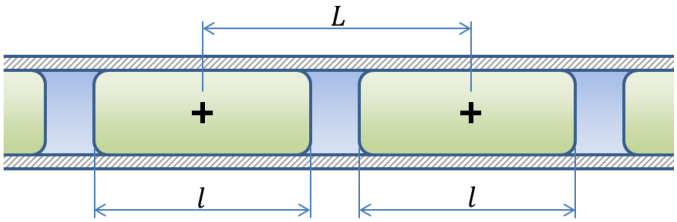

Figure 1: Geometric variables for a sequence of Taylor-bubbles

The relationship between the resonance frequency and the geometric variables for a sequence of Taylor-bubbles is given in equation (2) according to Han *et al.* (2011).

$$f_{res,Taylor} = \frac{1}{\pi \cdot l} \sqrt{\frac{\kappa \cdot p}{\rho_{liq} \cdot \left(\frac{L}{l} - 1\right)}} \tag{2}$$

Thus the resonance frequency according to equation (2) is no longer depending on the bubble diameters, but from the remaining dimensions L and l, where L is the distance between the center points of two consecutive Taylor-bubbles and l is the bubble length. Equation (2) is only valid, when the distance L is always larger than the length l, so that the thickness of the remaining fluid plug between two consecutive Taylor-bubbles is always larger than zero.

In the following experimental studies the oscillation of Taylor bubbles and the collapse of large bubbles passing an orifice are determined as a noise-inducing effect. The measured frequencies of the noise emitted by the Taylor-bubbles are consistent with the predictions according to equation (2). Furthermore they are lower than the resonance frequencies of corresponding spherical bubbles with the same volume. While passing an orifice the bubbles emit noises with resonance frequency of corresponding spherical bubbles of the same diameter like the orifice. An increase of the sound pressure level and acceleration amplitude was observed during the transition from slug flow to churn flow (Han *et al.*, 2011).

2.2. Sound perception and weighting

The sensitivity of the human ear depends on frequency and sound pressure level (DIN ISO 226, 2006). A higher sensitivity is given especially in the center frequency range (Möser, 2007). By A-weighting of the sound signal this fact is taken into account for all measured acoustic signals coming from structure born sound or airborne sound. A frequency-dependent sensitivity, comparable to the human hearing, is applied to each sensor. The specific damping rates for each frequency band are written in DIN EN 61672-1, 2014.

For quantifying noise events occurring primarily through a changing loudness, the corresponding level curve of each measured sound signal is converted. This take place for both sound pressure and acceleration signals, according to equation (3). The reference value for the sound pressure p_{ref} is 20 µPa (Möser, 2007) and for the acceleration a_{ref} is 1 µm/s² (Kollmann, 2006).

$$L(t) = 20 \cdot lg\left(\frac{x(t)}{x_{ref}}\right) \;\; mit \;\; x(t) = \begin{cases} p(t) \\ a(t) \end{cases}, \; x_{ref} = \begin{cases} p_{ref} \\ a_{ref} \end{cases} \tag{3}$$

A time-weighting of the signal amplitude is performed to detect the rapidly alternating noise level values. Therefore the signal is integrated by a sliding exponential averaging with a time constant of τ = 35 ms, both of the rising and falling sound pressure levels.

In order to get a clean frequency response from a non-periodic signal, leakage effects have to be avoided. Therefor a *Hann*-window function is applied over a finite interval with the duration T, according to equation (4). Thereby the amplitude is getting close to zero at the beginning and end of the interval. (Möser, 2007)

$$x(t) \rightarrow x_{hann}(t) = x(t) \cdot h(t) = x(t) \cdot \frac{1}{2}\left(1 - \cos\left(2\pi \frac{t}{T}\right)\right) \;\; mit \;\; x(t) = \begin{cases} p(t) \\ a(t) \end{cases} \tag{4}$$

3. EXPERIMENTAL INVESTIGATIONS

3.1. Test setup and measurement devices

The test setup in general is converted from a commercial bottom-freezer. Therefore original components are arranged in a supporting frame structure identical to the serial device. The accessibility of the refrigerant cycle is ensured by attaching adaptive modular insulation panels. The thermal insulation properties of the original used polyurethane foam are adjusted by adapting the ambient temperature. Therefore the test setup is installed in a environmental chamber. The deviation of the compartment's performance, compared to the performance of the serial device is low. To detect of the flow pattern two special made sight glasses are installed at the inlet and outlet of the freezers capillary tube. A detailed description of the experimental setup can be found in Tannert and Hesse (2013). The refrigerant used for the tests is isobutane (R600a).

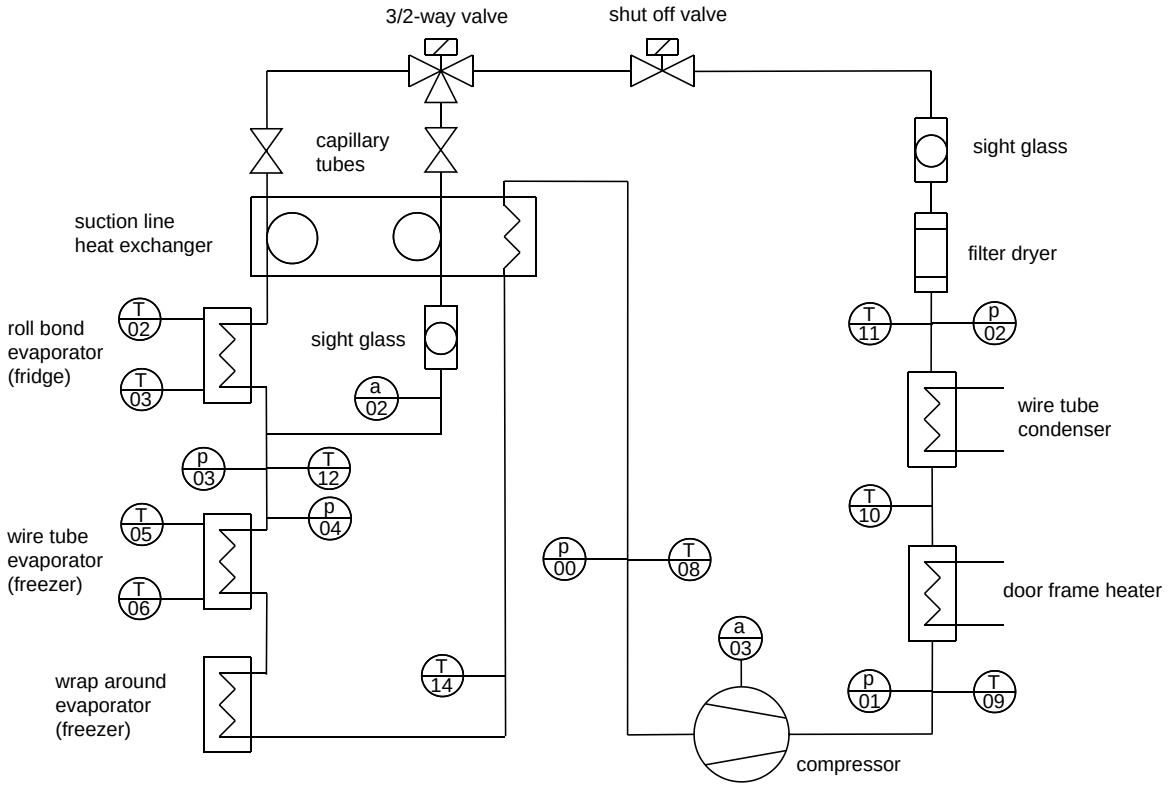

Figure 2: Flow chart of the test setup (Tannert and Hesse, 2014)

To measure the thermodynamic state variables of the cooling process, pressure transducers and temperature sensors (thermocouples) are installed all over the refrigeration cycle, especially before and behind the freezers capillary tube (see. Fig. 5). Additional to the static pressure signals, the dynamic pressure at the outlet of the freezers capillary tube is measured as well.

To identify the mass flow rate of the compressor it is necessary to record the compressor speed. Therefore an acceleration sensor is installed at the compressor housing. With a frequency analysis of the acceleration signal the rotational speed is determined. As can be seen later on, it has to be distinguished between the mass flow rate delivered by the compressor and the mass flow rate passing the capillary tube.

Airborne sound signals are recorded by two microphones. One is located close to the test setup's backside within the test chamber, the other one is placed inside the refrigerator compartment close to rollbond-evaporator. Preliminary investigations have shown that the noise, which is perceptible from the test setup outside, is mainly caused by the sound radiation of the rollbond-evaporator. Close to the freezers capillary tube outlet another acceleration sensor is attached on the tubing of the freezer evaporator for the acquisition of the structure-borne sound.

3.2. Data acquisition and flow visualization

To enable the detection of causal dependencies between the different measured variables, a time-synchronous data acquisition is necessary. a different sampling rate is used for every type of measured signal. Therefor the high-frequency signals (sound pressure, acceleration and dynamic pressure) are sampled at 12.8 kHz, temperature signals are sampled with 0.8 Hz and static pressure signals are sampled with 100 Hz. In addition, the electrical power consumption of the device is logged. A suitable data acquisition system is presented in Tannert and Hesse (2013).

The recording technique used for capturing images and video sequences is presented in Tannert and Hesse (2013) as well. The synchronization of the measured acoustical and thermodynamic signals with the video sequences is done by manually setting of an acoustic trigger at the beginning of each measurement. During the post-process this trigger can be identified in the acoustic signals and in the soundtrack of the video sequence.

3.3. Operational mode

To ensure comparable results of various measurements the data is always recorded during a characteristic operation mode. The test setup is operated with the electronic control device installed by the manufacturer. For the investigations presented in this paper the freezer mode was identified as the most critical mode (see. Figure 3), since the noise occurrence is most succinctly herein.

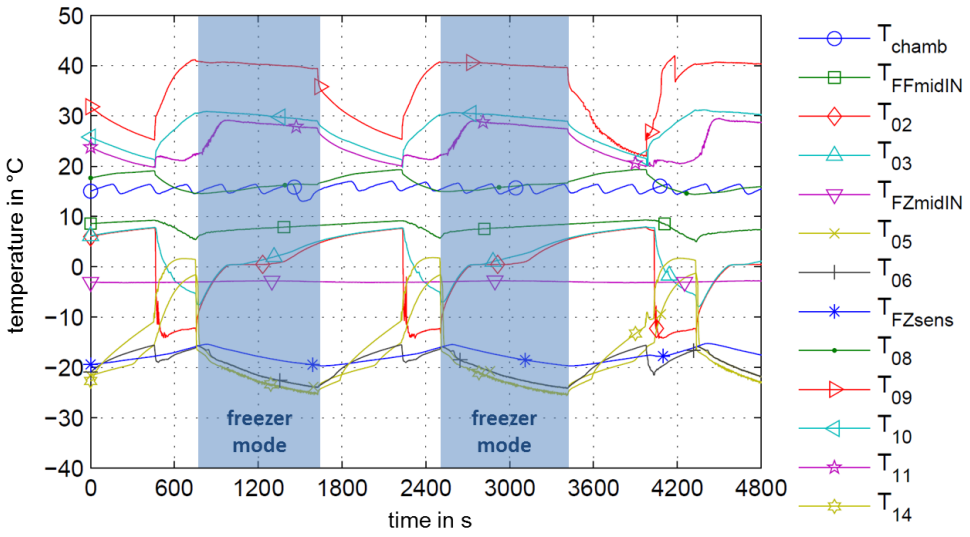

Figure 3: Operational mode of the test setup for data recording

The evaluation of the measured data is carried out towards the end of the operational mode. Then the refrigeration cycle runs most widely in a thermodynamic steady state and there is only a slight transient deviation in the signals.

4. RESULTS AND DISCUSSION

4.1. Flow-induced noise and its source

The evaluation of the acoustic sensor signals shows periodic fluctuation. This effect can be observed in the level curve of the acceleration signal, measured close to the freezers capillary tube outlet (red graph, Figure 4). The fluctuation is also visible in the level curve of the sound pressure signal coming from the microphone close to the rollbond-evaporator in the refrigerator compartment (green graph, Figure 4). And finally a simultaneously rise of the dynamic pressure signal amplitude recorded inside the refrigerant flow close to the freezers capillary tube outlet can be found (blue graph, Figure 4). The fluctuation in all signals is running synchronously.

The fluctuation of the sound pressure level and the acceleration level are characterized by a alternating sequence of high and low level value. At the beginning of the freezer mode the temporal portions of the high level noise predominates. During progression of the freezer mode the periodicity of the level fluctuation is concretized by increasing the temporal portions of the low noise level.

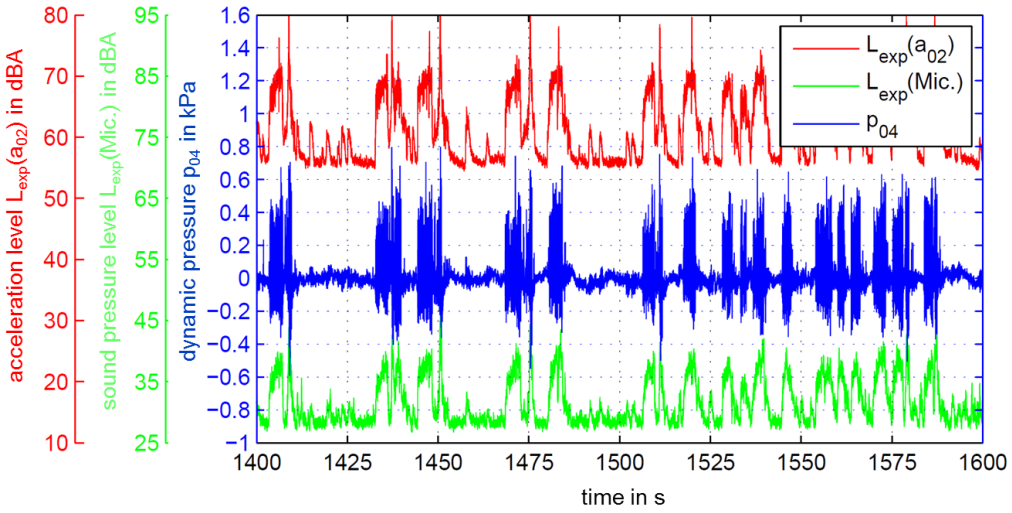

Figure 4: Fluctuation in the noise level signals and in the dynamic pressure signal

From the graphs of sound pressure level and acceleration level dependencies between different effects in the refrigeration cycle are obvious. The fluctuation of the sound pressure level recorded by the externally microphone (airborne sound) correlates to the fluctuation of the acceleration level (structure-borne sound) concerning intensity and periodicity. Coincidentally pressure pulsations occur with identical periodicity like the fluctuation of the sound pressure level and the acceleration level. Regarding the knowledge about the alternating flow pattern at the capillary tube outlet as stated in Tannert and Hesse (2013), it can be concluded, that the origin of flow induced noise is the refrigerant flow passing the capillary tube outlet. For the first step the propagation of induced sound cannot yet be clarified. Two different ways can be considered: On the one hand it can be assumed, that the sound is transmitted along the reverberant tubing structure. On the other hand it can be assumed that the sound is transmitted in the flowing medium (through the gas phase). In both cases other components (e.g., the rollbond-evaporator) can get excited to oscillations, whereby the radiation of airborne noise to the environment can be caused.

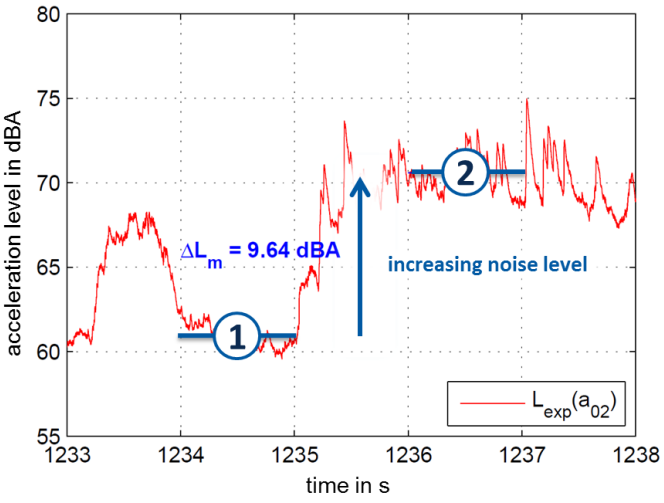

Figure 5: Equivalent continuous sound level values of the low noise level (time interval: 1234-1235s) and the high noise level (time interval: 1236-1237s) before and after a certain level skip

The abrupt change between the low and the high value of the noise level is called a level skip. For a short time interval before and after the level skip the equivalent continuous sound level is calculated from the A-weighted sound pressure level in both intervals (label 1 and 2 in Figure 5). The difference between the two equivalent continuous sound level values is called level skip value (see. Figure 5). The noise fluctuation of a specific operation

state is quantified by the average of several level skip values recorded within this operation state. Having the system run through different operation states allows a comparison of the noise fluctuation between these states.

To determine changes in the frequency response between low and high noise level, the signal waveform of the acceleration sensor in both intervals (low and high noise level) is superimposed with a *Hann*-window-function. Afterwards the time-weighted signals of both intervals are then transferred by means of Fourier analysis into the frequency domain. The frequency response will show significant increases in the amplitude for discrete frequencies respectively for certain frequency ranges, which cause the increase of the noise level (see. Figure 6).

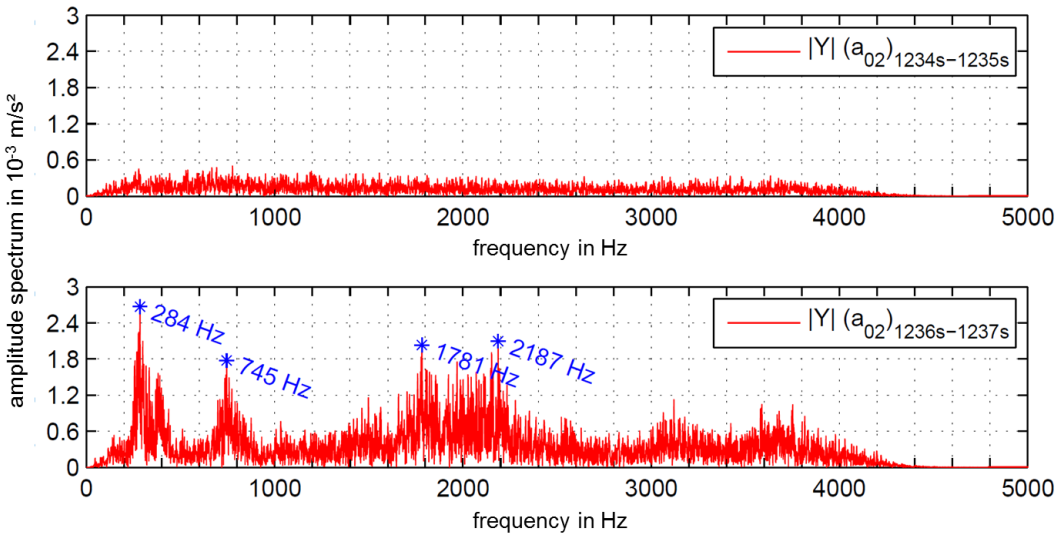

Figure 6: Frequency responses of the low noise level (time interval: 1234-1235s) and the high noise level (time interval: 1236-1237s) before and after a certain level skip

An increase of the amplitude can be found at certain single frequencies of about 280 Hz and 740 Hz as well as in a wide band around 2000 Hz. The increasing amplitudes of the frequency response can be reproduced through the analysis of several level skips during an operational state. As described in section 2. it can be assumed, that vapor bubbles of a certain geometry cause flow-induced noise. A verification of this theory can be done in the next step. Therefore the results of this frequency analysis and additional information about the bubble geometry coming out of the flow visualization will be used.

4.2. Local flow pattern visualization

From the visual observation of the refrigerant flow at the capillary tube inlet and outlet (regarding to Tannert and Hesse, 2013) a relationship between changes in the flow pattern at the capillary tube outlet and the alternating noise level can be determined. The alternating vapor mass fraction of the refrigerant flow entering the capillary tube does not correlate with the alternating noise level at the capillary tube outlet, even though a time delay between the flow pattern at the capillary tube inlet and the occurring noise effects is observable.

Two cases of refrigerant flow shapes leaving the capillary tube can be distinguished, depending on the refrigerant state at the capillary tube inlet: Initially the capillary tube inlet is flushed with liquid refrigerant. During the further process the liquid level above the capillary tube inlet (observable inside the filter dryer) decreases until initial gas or vapor enters the capillary tube. During this state the shape of the refrigerant flow at the capillary tube outlet can be described as an undisturbed free jet. The flow pattern is still a two-phase flow with a small and nearly constant vapor mass fraction. New studies with an improved lightning technique identify an annular flow in the end region of capillary tube (see. Figure 7, left) for this outflow state. Simultaneously occurring amplitude alterations of the dynamic pressure are not observable. The noise level measured by the acoustical sensors is at a low level.

The initial vapor entrainment at the capillary tube inlet reaches the capillary tube outlet. A sharp increase of the vapor mass fraction occurs and the refrigerant flow shape leaving the capillary tube outlet turns into a second

distinguishable state. A discontinuous free jet is resulting, characterized by a rapidly fluctuating vapor mass fraction. A plug flow can be identified in the end section of the capillary tube (see. Figure 7, right). In coincidence with the entrainment of refrigerant with fluctuating vapor mass fraction into the evaporator, both significant amplitude alterations of the dynamic pressure and an increase of the sound pressure and acceleration level can be measured.

In this way several specific flow pattern can be assigned to the specific state of low and high values of the noise level. Therefore the origin of the flow-induced noise can be found at the capillary tube outlet caused by the periodically changing flow pattern of the refrigerant.

Further observations of the refrigerant flow in the end section of the capillary tube show the occurrence of Taylor bubbles while the refrigerant flow pattern is plug flow (see. Figure 7, right). Based on the short-exposed images the characteristic geometries of the vapor bubbles can be determined according to the model description in section 2. Regarding the fluid properties the calculation of the associated resonant frequency is performed using Equation 2. The estimated resonance frequency is in the range of 280 Hz, which is in good agreement with the experimental results. Thus, the root cause of the flow-induced noise excitation has been proven, at least for a specific frequency.

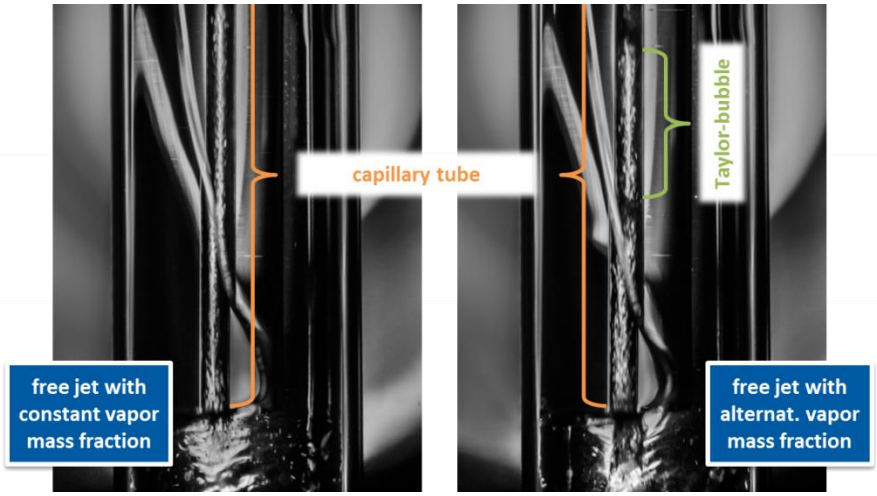

Figure 7: Refrigerant flow pattern in the end section of the capillary tube, left: annular flow, right: plug flow with Taylor bubbles

Going on from the origin the flow-induced noise can be transmitted through the fluid itself or along the piping structure. Through the sound conduction different components can easily get excited to oscillations and contributes to externally perceivable noise. The detectable fluctuation of the dynamic pressure, which occurs concurrently with the increasing noise level, demonstrates the sound conduction through the fluid. In comparison to this the measured acceleration of the evaporator tube shows the structural sound transmission. A superposition of both mechanisms can be considered as well.

5. CONCLUSION

Based on the results of previous studies concerning the flow pattern in capillary tubes of household refrigerators, noise effects occurring in the refrigeration cycle of household appliances are considered in this work. Starting from theoretical approaches concerning the basic root causes for the excitation of noise in the refrigerant flow, the required test setup is explained further as well as the post-processing of acoustic signals to validate the noise effects.

In the experimental investigation a simultaneous occurrence of fluctuation in the dynamic pressure and alterations of the noise level can be observed. The changing noise level can be quantified by determining the averaged difference of the equivalent continuous sound level value in intervals before and after a certain level skip. Throughout this characterization of noise effects various operating states can be distinguished. Furthermore the frequency response is analyzed for the low and high noise level intervals. Therefore amplitude increases can be detected for certain single frequencies and limited frequency bands during the occurrence of a high noise level.

By observing the refrigerant flow at the capillary tube inlet and outlet an alternating refrigerant flow at the capillary tube outlet can be determined. This occurs synchronously with the fluctuation of the dynamic pressure and the noise level. At a low noise level the flow regime of the refrigerant passing the capillary tube outlet can be described as free jet with constant vapor mass fraction. The flow pattern in the end section of the capillary tube is found to be an annular flow. The fluctuating vapor entrainment into the capillary tube leads to a rapidly alternating vapor mass fraction in the refrigerant free jet leaving the capillary tube outlet. This effect is associated with the simultaneous occurrence of a significant increasing noise level, determined from the measurement of the acoustic signals, as well as amplitude peaks of dynamic pressure, recorded inside the fluid behind the capillary tube outlet. Plug flow can be detected in the end section of the capillary tube.

Therefore the origin of the externally perceivable noise can be clearly identified as the capillary tube outlet. Regarding the measured fluctuation of the dynamic pressure, the noise excitation is found to be caused principally by the alteration of the refrigerant flow regime passing the capillary tube outlet. Representative Taylor bubbles can be observed within the plug flow. As mentioned in the theory, a resonance frequency can be calculated for this kind of bubble geometry. Matching values for the resonance frequency can be achieved between the theoretical approach and a certain frequency derived from the noise measurement. Thus the mechanism of the flow-induced noise excitation can be clarified to some extent throughout the presented investigation. Additional the sound transmission between the origin of excitation and the point of emission is rudimentary discussed.

Further investigations deal with the influence of these local state changes shown here on the dynamics of the entire refrigeration system. The mechanism for flow-induced noise has to be discussed in detail regarding the remaining frequencies, which contribute to the increasing amplitude of the high noise level. Finally, different methods are to be discussed and experimentally validated, which may prevent instabilities of the capillary tube flow as shown here.

NOMENCLATURE

a(t)	acceleration curve	(m/s^2)
d	bubble diameter	(m)
f	resonance frequency	(Hz)
κ	polytrophic exponent	(-)
L	center-distance	(m)
L(t)	sound pressure level / acceleration level	(dBA)
ΔL	difference of acceleration level	(dBA)
l	bubble length	(m)
p(t)	pressure curve	(bar)
t	time	(s)
T	temperature	(°C)
|Y|	amplitude spectrum	(m/s^2)
ρ	density	(kg/m^3)
x(t)	signal curve, general	(-)

Subscript

00…14	index number of sensor
chamb	test chamber
exp	exponential averaged
FFmidIN	fresh food compartment
FZmidIN	freezer compartment
FZsens	freezer compartment appliance sensor
hann	*Hann*-window function
liq	liquid
m	equivalent continuous
ref	reference
res	resonance
spherical	spherical shaped bubble
Taylor	Taylor-bubble

REFERENCES

DIN Deutsches Institut für Normung e.V., 2006, *DIN ISO 226 Akustik - Normalkurven gleicher Lautstärkepegel*, Beuth Verlag GmbH, Berlin.

DIN Deutsches Institut für Normung e.V., 2014, *DIN EN 61672-1 Elektroakustik - Schallpegelmesser - Teil 1: Anforderungen*, Beuth Verlag GmbH, Berlin.

Han, H.S., Jeong, W.B., Kim, M.S., Kim, T.H., 2009, Analysis of the root causes of refrigerant-induced noise in refrigerators, *Journal of mechanical science and technology*, vol. 23: p. 3245-3256.

Han, H.S., Jeong, W.B., Kim, M.S., Lee, S.Y., Seo, M.Y., 2010, Reduction of the refrigerant-induced noise from the evaporator-inlet pipe in a refrigerator, *Int. J. Refrig.*, vol. 33: p. 1478-1488.

Han, H.S., Jeong, W.B., Kim, M.S., 2011, Frequency characteristics of the noise of R600a refrigerant flowing in a pipe with intermittent flow pattern, *Int. J. Refrig.*, vol. 34: p. 1498-1506.

Hartmann, D., Melo, C., 2012, Popping Noise in Household Refrigerators: Fundamentals and Practical Solutions, *Int. Refrig. and Air Cond. Conf.*, Purdue: 2147 p. 1-10.

Kollmann, F.G., Schösser, T.F., Angert, R., 2006, *Praktische Maschinenakustik*, Springer, Berlin, Heidelberg, 363 p.

Minnaert, M., 1933, On musical air-bubbles and the sounds of running water, *Philosophical Magazine Series 7*, p. 235-248.

Möser, M., 2007, *Technische Akustik*, Springer, Berlin, Heidelberg, New York, 539 p.

Simoes-Moreiraa, J.R., Bullard, C.W., 2003, Pressure drop and flashing mechanism in refrigerant expansion devices, *Int. J. Refrig.*, vol. 26: p. 840-848.

Tannert, T., Hesse, U., 2013, Zweiphasige Kältemittelströmung in Kapillarrohren an Haushaltkältegeräten. *DKV-Jahrestagung 2013*, DKV e.V., Hannover.